Ph.D. in Information and Communication Engineering

Ph.D. Course on

Analytical Techniques for Wave Phenomena

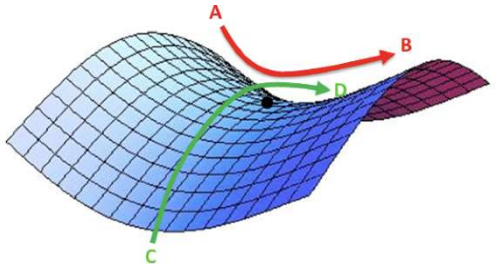

Lesson 12

Paolo Burghignoli

SAPIENZA
UNIVERSITÀ DI ROMA

Dipartimento di Ingegneria dell'Informazione, Elettronica e Telecomunicazioni

Plane-Wave Scattering from a Sphere

The Configuration

Let us consider a **uniform plane wave**, propagating along the z-axis with an x-polarized electric field, **impinging on a PEC sphere**

$$E_x^{\mathrm{i}} = E_0^{\mathrm{i}} e^{-jkr\cos\theta}$$

$$H_y^{\mathrm{i}} = \frac{E_0^{\mathrm{i}}}{\zeta} e^{-jkr\cos\theta}$$

For convenience in applying boundary conditions, we wish to express this field as the sum of components TM and TE to r.

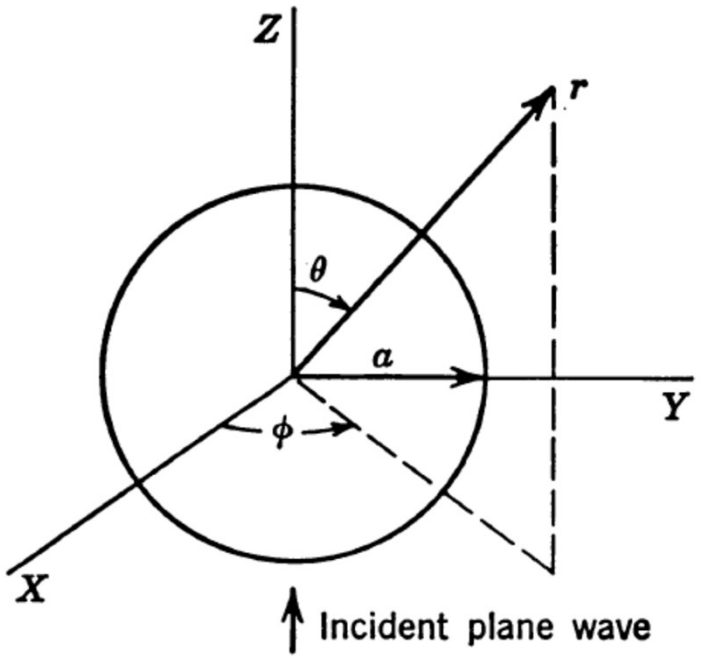

TM^r-TE^r Decomposition of the Incident Field

The r component of $\mathbf{E}^{\mathrm{i}}$ is

$$
\begin{aligned}
E_r^{\mathrm{i}} &= \cos\phi \sin\theta E_x^{\mathrm{i}} = E_0^{\mathrm{i}} \frac{\cos\phi}{jkr} \frac{\partial}{\partial\theta}\left(e^{-jkr\cos\theta}\right) \\
&= E_0^{\mathrm{i}} \frac{\cos\phi}{jkr} \sum_{n=0}^{+\infty} j^{-n}\left(2n+1\right) j_n\left(kr\right) \frac{\partial}{\partial\theta} P_n\left(\cos\theta\right) \\
&= E_0^{\mathrm{i}} \frac{\cos\phi}{jkr} \sum_{n=0}^{+\infty} j^{-n}\left(2n+1\right) j_n\left(kr\right)\left(-\sin\theta\right) \frac{\partial P_n\left(\cos\theta\right)}{\partial\cos\theta} \\
&= -jE_0^{\mathrm{i}} \frac{\cos\phi}{\left(kr\right)^2} \sum_{n=0}^{+\infty} j^{-n}\left(2n+1\right) \hat{J}_n\left(kr\right) P_n^1\left(\cos\theta\right)
\end{aligned}
$$

where we have used the property

$$
P_\nu^m\left(x\right) = \left(-1\right)^m \left(1-x^2\right)^{m/2} \frac{\mathrm{d}^m P_m\left(x\right)}{\mathrm{d}x^m}
$$

TM^r-TE^r Decomposition of the Incident Field

We thus construct the radially directed magnetic potential as

$$A_r^{\mathrm{i}} = E_0^{\mathrm{i}} \frac{\cos\phi}{k\zeta} \sum_{n=0}^{+\infty} a_n \hat{J}_n\left(kr\right) P_n^1\left(\cos\theta\right)$$

Recalling that

$$E_r = \frac{1}{j\omega\varepsilon_{\mathrm{c}}}\left(\frac{\partial^2}{\partial r^2} + k^2\right) A_r \qquad \left[\frac{\mathrm{d}^2}{\mathrm{d}r^2} + k^2 - \frac{\nu\left(\nu+1\right)}{r^2}\right] \hat{J}_\nu\left(kr\right) = 0$$

we find

$$E_r^{\mathrm{i}} = -jE_0^{\mathrm{i}} \frac{\cos\phi}{\left(kr\right)^2} \sum_{n=0}^{+\infty} a_n n\left(n+1\right) \hat{J}_n\left(kr\right) P_n^1\left(\cos\theta\right)$$

TM^r-TE^r Decomposition of the Incident Field

Comparing with the previous expression, we obtain

$$a_n = \frac{j^{-n}\left(2n+1\right)}{n\left(n+1\right)}$$

A similar procedure using H_r^{i} and F_r^{i} gives

$$F_r^{\mathrm{i}} = E_0^{\mathrm{i}} \frac{\sin\phi}{k} \sum_{n=0}^{+\infty} a_n \hat{J}_n\left(kr\right) P_n^1\left(\cos\theta\right)$$

with the same coefficients a_n as those already found for A_r^{i} .

Scattered and Total Potentials

The **scattered potential** is then expressed through radially outgoing functions:

$$A_r^{\mathrm{s}} = -E_0^{\mathrm{i}} \frac{\cos\phi}{k\zeta} \sum_{n=0}^{+\infty} b_n \frac{j^{-n}\left(2n+1\right)}{n\left(n+1\right)} \hat{H}_n^{(2)}\left(kr\right) P_n^1\left(\cos\theta\right)$$

$$F_r^{\mathrm{s}} = -E_0^{\mathrm{i}} \frac{\sin\phi}{k} \sum_{n=0}^{+\infty} c_n \frac{j^{-n}\left(2n+1\right)}{n\left(n+1\right)} \hat{H}_n^{(2)}\left(kr\right) P_n^1\left(\cos\theta\right)$$

so that the **total** potentials are

$$A_r = E_0^{\mathrm{i}} \frac{\cos\phi}{k\zeta} \sum_{n=0}^{+\infty} \frac{j^{-n}\left(2n+1\right)}{n\left(n+1\right)} \left[\hat{J}_n\left(kr\right) - b_n \hat{H}_n^{(2)}\left(kr\right)\right] P_n^1\left(\cos\theta\right)$$

$$F_r = E_0^{\mathrm{i}} \frac{\sin\phi}{k} \sum_{n=0}^{+\infty} \frac{j^{-n}\left(2n+1\right)}{n\left(n+1\right)} \left[\hat{J}_n\left(kr\right) - c_n \hat{H}_n^{(2)}\left(kr\right)\right] P_n^1\left(\cos\theta\right)$$

Enforcing the Boundary Conditions

By enforcing the **vanishing of the tangential components** of the electric field on the surface $r = a$ of the PEC sphere, it is readily found that

$$b_n = \frac{\hat{J}_n'(ka)}{\hat{H}_n^{(2)'}(ka)}$$

$$c_n = \frac{\hat{J}_n(ka)}{\hat{H}_n^{(2)}(ka)}$$

Plane-Wave Scattering from a Transparent Sphere

The same approach can be adopted for treating plane-wave scattering from a **homogeneous isotropic sphere** characterized by the consitutitve parameters ε_{d}, μ_{d}.

In this case, there is also a **transmitted field** inside the sphere, which can be expressed in terms of the potentials

$$A_r^{\mathrm{t}} = E_0^{\mathrm{i}} \frac{\cos\phi}{k\zeta} \sum_{n=0}^{+\infty} \frac{j^{-n}\left(2n+1\right)}{n\left(n+1\right)} d_n \hat{J}_n\left(k_{\mathrm{d}} r\right) P_n^1\left(\cos\theta\right)$$

$$F_r^{\mathrm{t}} = E_0^{\mathrm{i}} \frac{\sin\phi}{k} \sum_{n=0}^{+\infty} \frac{j^{-n}\left(2n+1\right)}{n\left(n+1\right)} e_n \hat{J}_n\left(k_{\mathrm{d}} r\right) P_n^1\left(\cos\theta\right)$$

where $k_{\mathrm{d}} = \omega\sqrt{\mu_{\mathrm{d}}\varepsilon_{\mathrm{d}}}$ is the wavenumber inside the sphere.

Plane-Wave Scattering from a Transparent Sphere

By enforcing the **continuity of the tangential components** of both the electric and the magnetic field on the surface of the sphere, the coefficients b_n, c_n, d_n, and e_n can be found.

The final result for b_n and c_n is

$$b_n = \frac{-\sqrt{\varepsilon_{\mathrm{d}}\mu_0}\hat{J}_n'\left(ka\right)\hat{J}_n\left(k_{\mathrm{d}}a\right)+\sqrt{\varepsilon_0\mu_{\mathrm{d}}}\hat{J}_n\left(ka\right)\hat{J}_n'\left(k_{\mathrm{d}}a\right)}{\sqrt{\varepsilon_{\mathrm{d}}\mu_0}\hat{H}_n^{(2)'}\left(ka\right)\hat{J}_n\left(k_{\mathrm{d}}a\right)-\sqrt{\varepsilon_0\mu_{\mathrm{d}}}\hat{H}_n^{(2)}\left(ka\right)\hat{J}_n'\left(k_{\mathrm{d}}a\right)}$$

$$c_n = \frac{-\sqrt{\varepsilon_{\mathrm{d}}\mu_0}\hat{J}_n\left(ka\right)\hat{J}_n'\left(k_{\mathrm{d}}a\right)+\sqrt{\varepsilon_0\mu_{\mathrm{d}}}\hat{J}_n'\left(ka\right)\hat{J}_n\left(k_{\mathrm{d}}a\right)}{\sqrt{\varepsilon_{\mathrm{d}}\mu_0}\hat{H}_n^{(2)}\left(ka\right)\hat{J}_n'\left(k_{\mathrm{d}}a\right)-\sqrt{\varepsilon_0\mu_{\mathrm{d}}}\hat{H}_n^{(2)'}\left(ka\right)\hat{J}_n\left(k_{\mathrm{d}}a\right)}$$

Note that the PEC case can be recovered by letting $\mu_d \to 0 \quad \varepsilon_d \to \infty$ such that $k_{\mathrm{d}} = \omega\sqrt{\mu_d\varepsilon_d}$ remains finite.

Far Scattered Field

The **far scattered field** can be found using the asymptotic formula

$$\hat{H}_n^{(2)}\left(kr\right) \underset{kr\to\infty}{\sim} j^{n+1}e^{-jkr}$$

and retaining only the terms that vary as $1/r$. The result is

$$E_\theta^{\mathrm{s}} = -j\frac{E_0^{\mathrm{i}}}{kr}e^{-jkr}\cos\phi S_2\left(\beta,\theta\right)$$
$$E_\phi^{\mathrm{s}} = j\frac{E_0^{\mathrm{i}}}{kr}e^{-jkr}\sin\phi S_1\left(\beta,\theta\right)$$

where $\beta{=}ka$ and $S_{1,2}(\beta,\theta)$ are the so-called **amplitude functions** for the perpendicular and parallel polarizations, respectively, given by

The Mie Series

$$S_1\left(\beta,\theta\right)=\sum_{n=0}^{+\infty}\frac{\left(2n+1\right)}{n\left(n+1\right)}\left[-b_n\frac{P_n^1\left(\cos\theta\right)}{\sin\theta}+c_n\sin\theta P_n^{1'}\left(\cos\theta\right)\right]$$

$$S_2\left(\beta,\theta\right)=\sum_{n=0}^{+\infty}\frac{\left(2n+1\right)}{n\left(n+1\right)}\left[b_n\sin\theta P_n^{1'}\left(\cos\theta\right)-c_n\frac{P_n^1\left(\cos\theta\right)}{\sin\theta}\right]$$

This form of the solution is usually referred to as the **Mie series**

after Gustav Mie, who studied in 1908 plane-wave scattering by spherical particles in order to explain plasmon resonance in gold colloids:

[G. Mie, "Beiträge zur Optik trüber Medien, speziell kolloidaler Metallösungen" [Contributions to the optics of turbid media, particularly of colloidal metal solutions]. *Annalen der Physik* (in German), vol. 25, no. IV, pp. 377–445, 1908.]

The Mie Series

Alternatively, the Mie series can also be written as

$$S_1\left(\beta,\theta\right)=\frac{1}{2}\sum_{n=1}^{+\infty}\left(1-S_n^{(1)}\left(\beta\right)\right)t_n\left(\cos\theta\right)+\left(1-S_n^{(2)}\left(\beta\right)\right)p_n\left(\cos\theta\right)$$

$$S_2\left(\beta,\theta\right)=\frac{1}{2}\sum_{n=1}^{+\infty}\left(1-S_n^{(2)}\left(\beta\right)\right)t_n\left(\cos\theta\right)+\left(1-S_n^{(1)}\left(\beta\right)\right)p_n\left(\cos\theta\right)$$

with the angular factors defined as

$$p_n\left(\cos\theta\right)=\frac{2n+1}{n\left(n+1\right)}\frac{P_n^1\left(\cos\theta\right)}{\sin\theta}$$

$$t_n\left(\cos\theta\right)=-\frac{2n+1}{n\left(n+1\right)}\sin\theta P_n^{1'}\left(\cos\theta\right)$$

The Mie Series

and, for a **dielectric sphere** with $\varepsilon_{\mathrm{d}} = \varepsilon_0 N^2, \quad \mu_{\mathrm{d}} = \mu_0$:

$$S_n^{(1)}\left(\beta\right) = -\frac{\hat{H}_n^{(1)}\left(ka\right)}{\hat{H}_n^{(2)}\left(ka\right)} \frac{\ln' \hat{H}_n^{(1)}\left(ka\right) - N \ln' \hat{J}_n\left(k_{\mathrm{d}} a\right)}{\ln' \hat{H}_n^{(2)}\left(ka\right) - N \ln' \hat{J}_n\left(k_{\mathrm{d}} a\right)}$$

$$S_n^{(2)}\left(\beta\right) = -\frac{\hat{H}_n^{(1)}\left(ka\right)}{\hat{H}_n^{(2)}\left(ka\right)} \frac{N \ln' \hat{H}_n^{(1)}\left(ka\right) - \ln' \hat{J}_n\left(k_{\mathrm{d}} a\right)}{N \ln' \hat{H}_n^{(2)}\left(ka\right) - \ln' \hat{J}_n\left(k_{\mathrm{d}} a\right)}$$

where the *logarithmic derivative* is defined as

$$\ln' f\left(x\right) = \frac{\mathrm{d}}{\mathrm{d}x} \ln f\left(x\right) = \frac{f'\left(x\right)}{f\left(x\right)}$$

Exercise: show that the two alternative forms of the Mie series are equivalent.

PEC Sphere: Scattering Cross Section

Consider the backscattered field from a PEC sphere:

$$E_x^{\mathrm{s}} = E_\theta^{\mathrm{s}}\Big|_{\substack{\theta=\pi \\ \phi=\pi}} = E_\phi^{\mathrm{s}}\Big|_{\substack{\theta=\pi \\ \phi=-\pi/2}}$$

Using the Mie solution, we may calculate the (**back)scattering cross-section** (or **echo area**)

$$A_{\mathrm{e}} = \lim_{r\to+\infty}\left(4\pi r^2\left|\frac{E_x^{\mathrm{s}}}{E_0^{\mathrm{i}}}\right|^2\right)$$

$$= \frac{\lambda^2}{4\pi}\left|\sum_{n=1}^{+\infty}\frac{(-1)^n(2n+1)}{\hat{H}_n^{(2)}(ka)\,\hat{H}_n^{(2)\prime}(ka)}\right|^2$$

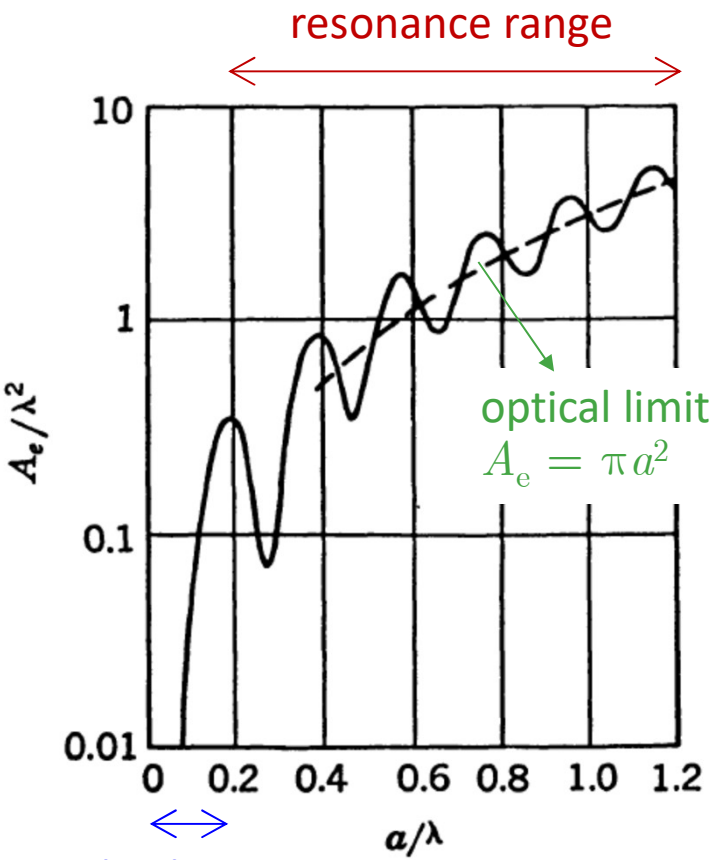

Plane-Wave Scattering from a Sphere: High-Frequency Asymptotics

The Localization Principle

Let us now consider the **high-frequency asymptotics** of the exact solution, i.e., the domain defined by the condition

$$\beta \doteq ka \gg 1$$

which is tantamount to $2a \gg \lambda$

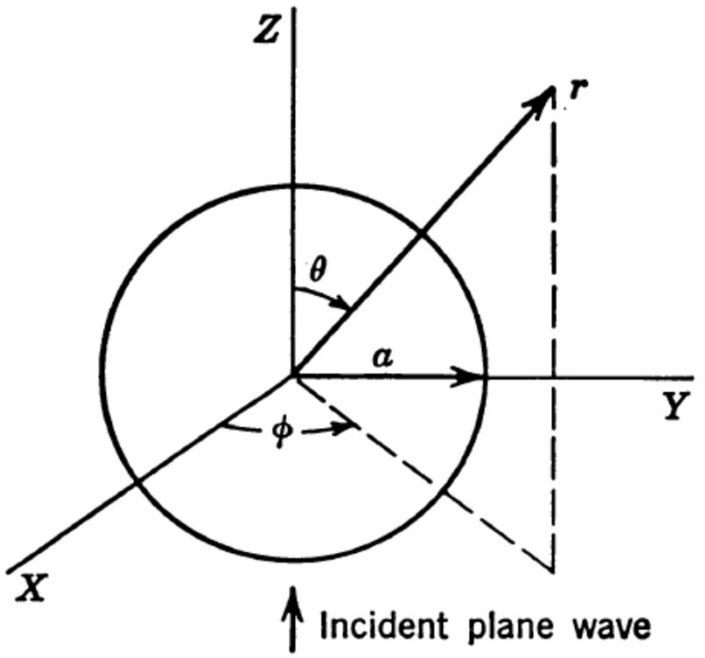

In this limit the incident plane wavefront may be thought to consist of **separate rays** which pursue their own path (**localization principle**).

The Localization Principle

A small part of a wide wave front can be looked upon as defining a ray which has for some length its own existence independent of the entire wave front. A length l requires a width D of the order of $\sqrt{l\lambda}$, and the requirement for any separate existence at all is a width $D > \lambda$.

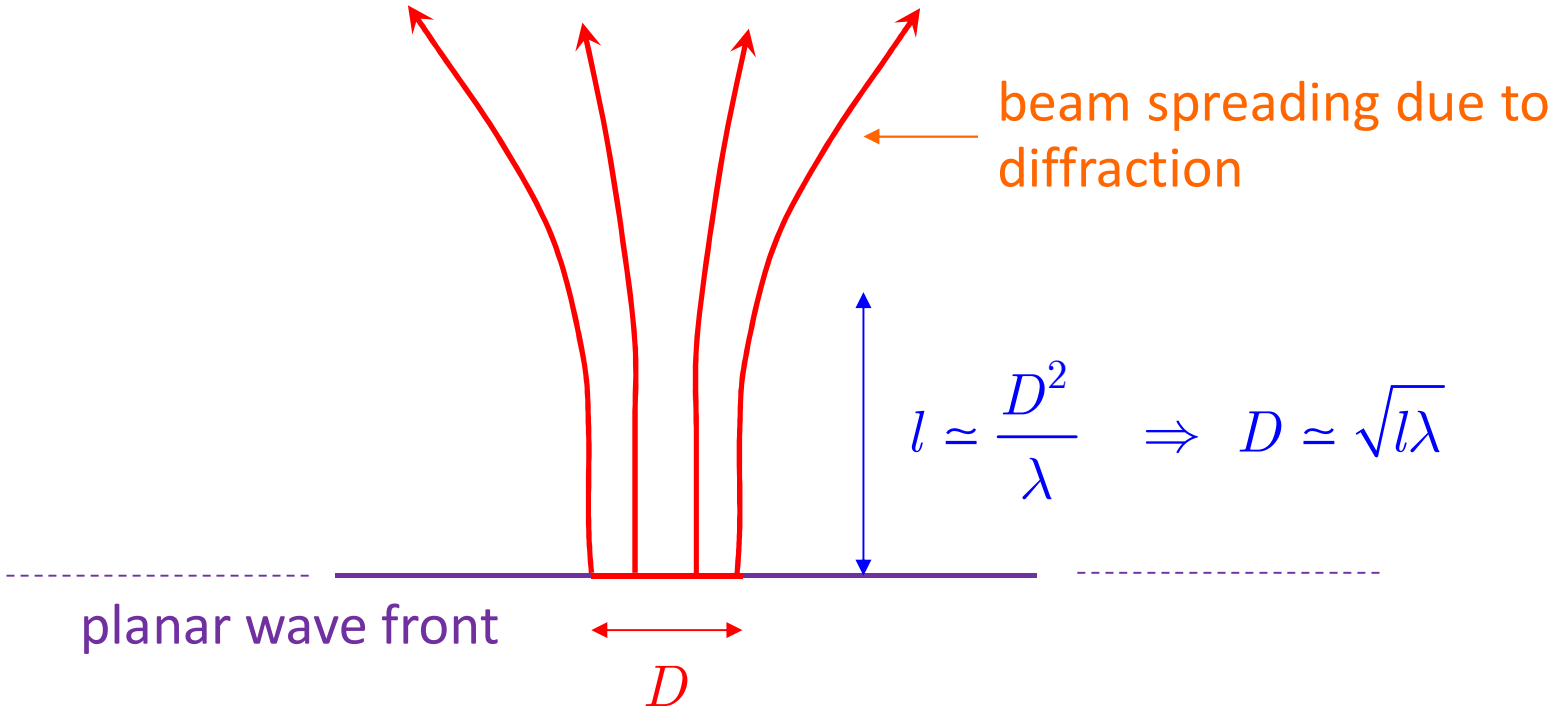

Impact Parameter

An asymptotic analysis of the n-th term of the Mie series shows that it corresponds to a ray passing the origin at a distance p_n (the **impact parameter**)

$$p_n = \left(n + \frac{1}{2}\right)\frac{\lambda}{2\pi}$$

When $\left(n+1/2\right) < \beta$ the rays **hit the sphere** and the spherical Bessel functions have an **oscillating** character.

When $\left(n+1/2\right) > \beta$ the rays **do not hit the sphere** and the spherical Bessel functions have an **exponentially decreasing** behavior as $n-\beta$ increases.

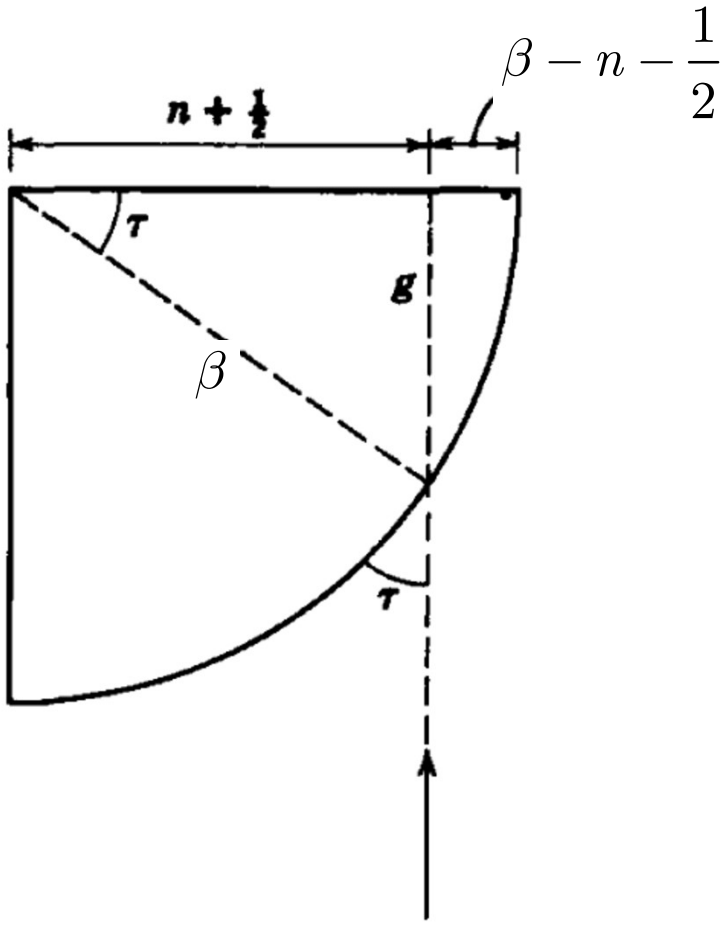

The Watson Transformation

The Watson transformation starts by rewriting a partial-wave series such as the Mie series as a **contour integral** around the positive half-axis of the s plane , where $s = n + 1/2$ is the "*complex angular momentum*"

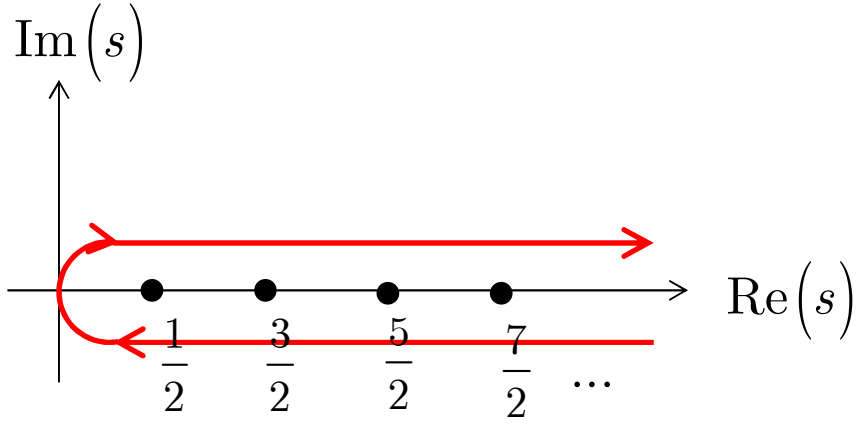

One then looks for a **deformation** (depending on the problem) such that the **dominant high-frequency contributions** to the resulting expression arise from the neighborhood of a small number of "**critical points**" (e.g., **saddle points** or **singularities** swept through in the deformation process such as poles, branch points).

PEC Sphere: Contribution of Critical Points

- A **real saddle point** $\overline{s}$ in the range $0 \le \overline{s} \le \beta$ corrresponds to a **ray** that hits the sphere at the impact parameter

$$p = \frac{\overline{s}}{k}$$

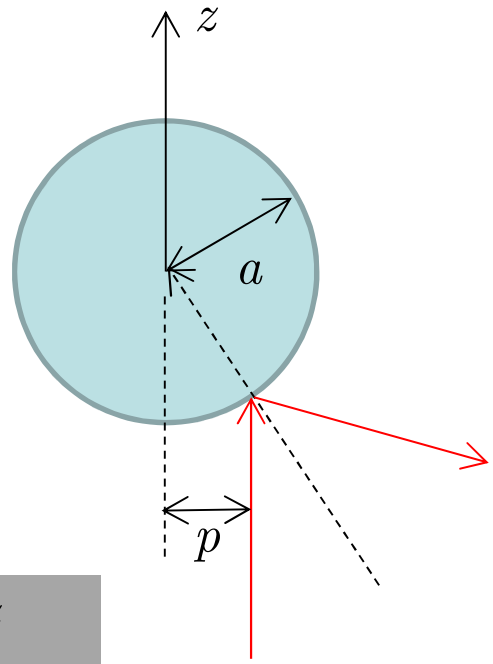

- **Complex** (Regge) **poles** correspond to **creeping waves** that penetrate the shadow region.

The imaginary part of the poles, which determines damping, increases rapidly, leading to a **rapidly convergent residue series** in the deep shadow region.

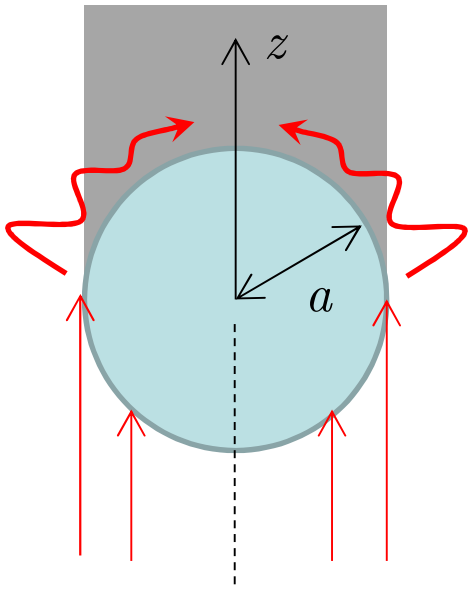

PEC Sphere: Transition Regions

The **transition** from the lit to the shadow sides of the sphere surface was studied by V. A. Fock in the 1940s.

It corresponds to the transition from a region where a real saddle point provides the dominant high-frequency contribution (*the lit side*) to a region with no real saddle points (*the shadow side*).

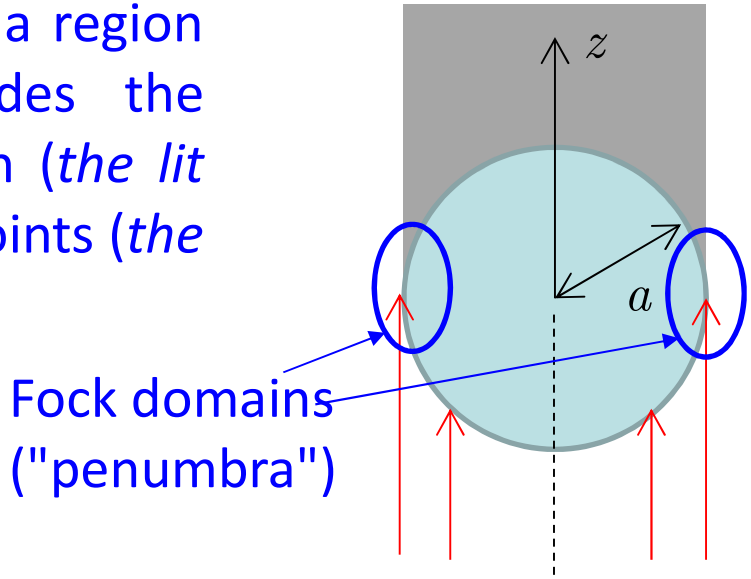

Modified Watson Transformation

In 1965, the Brazilian physicist H. M. Nussenzveig investigated plane-wave scattering from a PEC sphere using a modified form of the Watson transformation, based on the so-called **Poisson sum formula**:

$$\sum_{n=0}^{+\infty} \phi\left(n+\frac{1}{2},\mathbf{r}\right) = \sum_{m=-\infty}^{+\infty} \left(-1\right)^m \int_0^{+\infty} \phi\left(\lambda,\mathbf{r}\right) e^{j2m\pi\lambda} \mathrm{d}\lambda$$

where the interpolating function $\phi\left(\lambda,\mathbf{r}\right)$ reduces to $\phi\left(n+\frac{1}{2},\mathbf{r}\right)$ at the physical points.

Exploiting the symmetries of the integrand, the integral is extended to the entire real axis and then suitably deformed, as already described.

In contrast to the standard one, this modified form leads to convergent representations in **all the angular regions** around the sphere.

Dielectric Sphere

If the sphere is penetrable, the waves get inside, leading to *resonance effects* with much *weaker damping*. Correspondingly, **many Regge poles are located close to the real axis**, spoiling the rapid convergence.

In order to recover it, the solution must be rewritten in terms of **surface interactions**, as is done in the multiple-reflection treatment of Fabry-Perot interferometer.

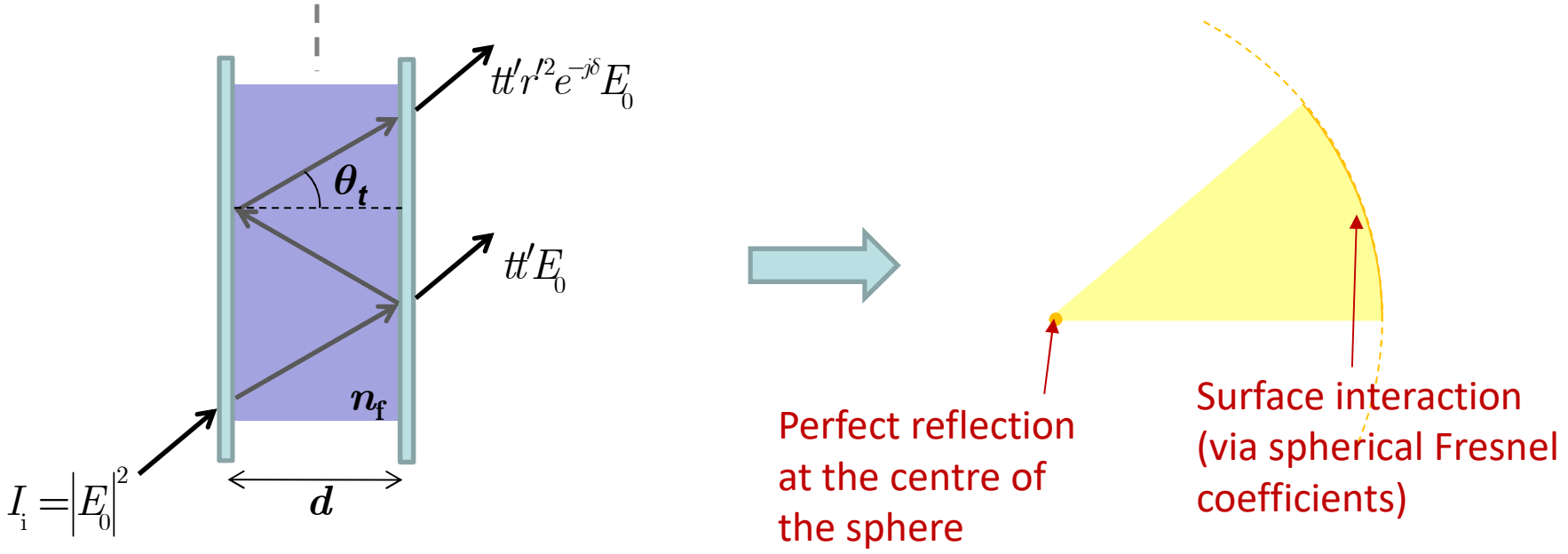

Debye Expansion

The resulting expression is known as the **Debye expansion**.

$$S_n^j(\beta) = \frac{\hat{H}_n^{(1)}(ka)}{\hat{H}_n^{(2)}(ka)} R_{22}^j + \frac{\hat{H}_n^{(1)}(ka)}{\hat{H}_n^{(2)}(ka)} \frac{\hat{H}_n^{(2)}(k_\mathrm{d}a)}{\hat{H}_n^{(1)}(k_\mathrm{d}a)} T_{21}^j T_{12}^j \left(\sum_{p=1}^{P} \rho_j^{p-1} + \frac{\rho_j^P}{1-\rho_j} \right)$$

$$\rho_j = \frac{\hat{H}_n^{(2)}(k_\mathrm{d}a)}{\hat{H}_n^{(1)}(k_\mathrm{d}a)} R_{11}^j$$

spherical reflection and transmission coefficients between region 1 (inside the sphere) and 2 (outside)

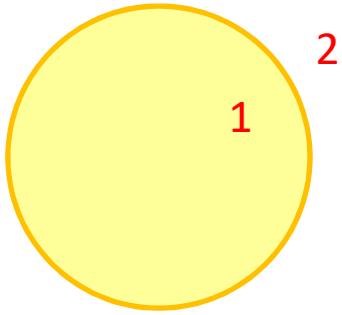

Debye Expansion

so that the scattering amplitudes are expressed as

$$S_j\left(\beta,\theta\right) = S_{j,0}\left(\beta,\theta\right) + \sum_{p=1}^{P} S_{j,p}\left(\beta,\theta\right) + \text{remainder}$$

direct reflection from the surface

transmission after $(p-1)$ **internal reflections**

By applying the modified Watson transformation to each term in the Debye expansion, the complex (Regge-Debye) poles are all associated to **rapidly damped creeping waves**, leading to **rapidly convergent asymptotic expansions**.

Dielectric Sphere: Critical Points for the Debye Expansion

- A **real saddle point** $\overline{s}$ in the range $0 \le \overline{s} \le \beta$ for the p-th Debye term corrresponds to a **ray** that hits the sphere at the impact parameter

$$q = \frac{\overline{s}}{k}$$

and undergoes $(p-1)$ internal reflections

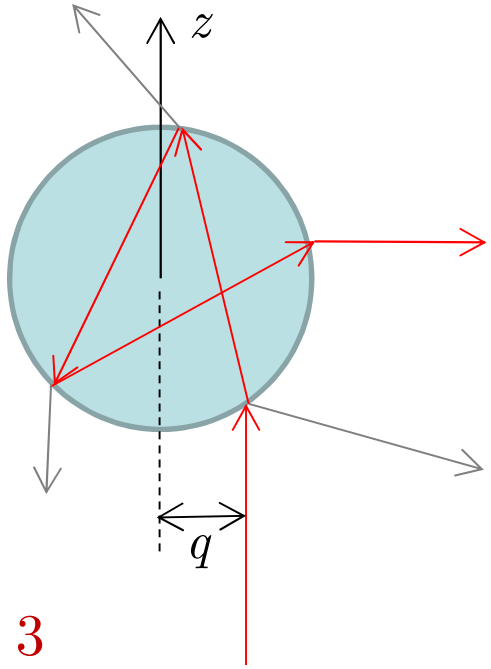

Example with $p = 3$

Dielectric Sphere: Critical Points for the Debye Expansion

- **Complex** (Regge-Debye) **poles** again correspond to **creeping waves** excited by tangentially incident rays.

In contrast with the impenetrable sphere, such waves not only travel around the sphere shedding diffracted rays but also **undergo critical refraction** inside the sphere, taking "shortcuts" through it…

For the p-th Debye terms there are p shortcuts.

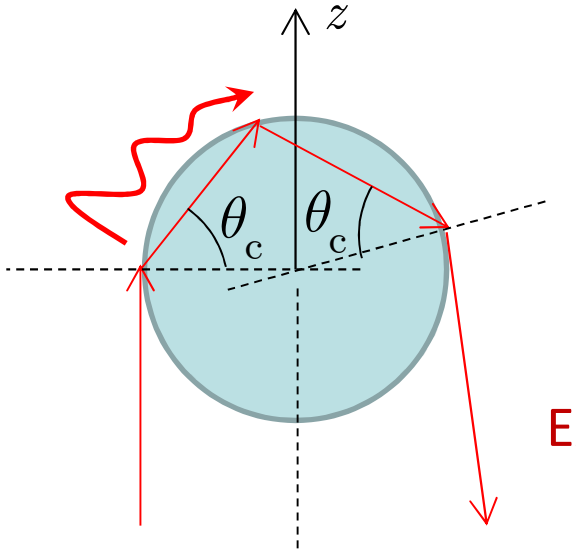

Example with $p = 2$

$$\theta_c = \sin^{-1}\left(\frac{1}{N}\right)$$

critical angle

Dielectric Sphere: Transition Regions

- A common transition region is associated with the **disappearance of one real ray** (a saddle point is replaced by a set of Regge-Debye poles): a Fock-type transition, as for PEC spheres

- Another transition region occcurs near the angles at which the scattering angle, as a function of the impact parameter, goes through an extremum: this is the **rainbow**.

- A different kind of transition region can be found *near the backscattering direction* ($\theta = \pi$), giving rise to the **glory**.

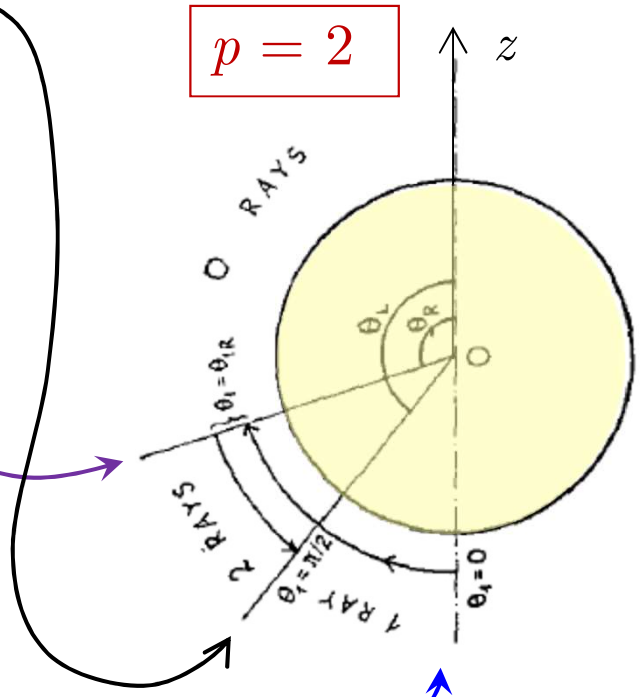

The Rainbow

The Main Features

The bright, inner band is the **primary bow.**

It is separated from the fainter **secondary bow** by a region, called **Alexander's dark band**, that is noticeably darker than the surrounding sky.

Below the primary bow are a few faint stripes of pink and green; they are **supernumerary arcs**.

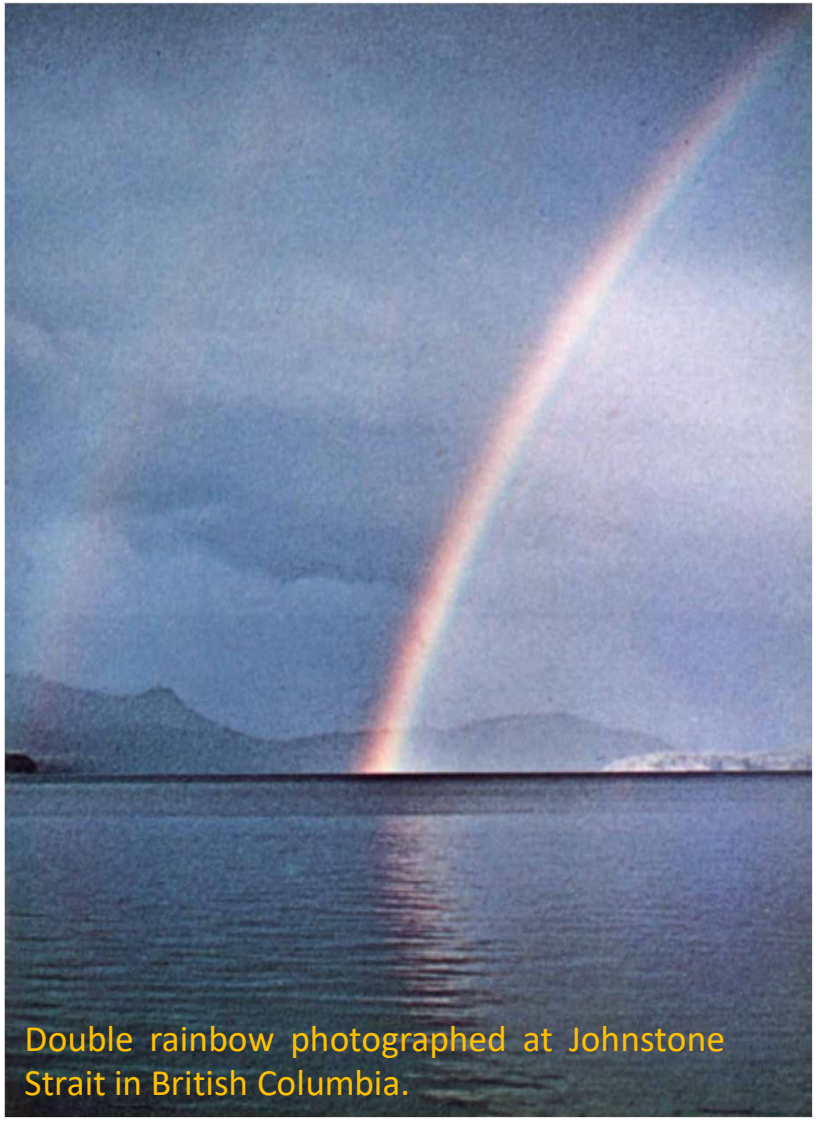

Double rainbow photographed at Johnstone Strait in British Columbia.

Geometry of the Rainbow

The geometry of the rainbow is determined by the **scattering angle**: the total angle through which a ray of sunlight is bent by its passage through a raindrop.

Rays are **strongly scattered** at angles of **138** degrees and **130** degrees, giving rise respectively to the *primary* and the *secondary rainbows*.

Between those angles **very little light is deflected**; that is the region of *Alexander's dark band*.

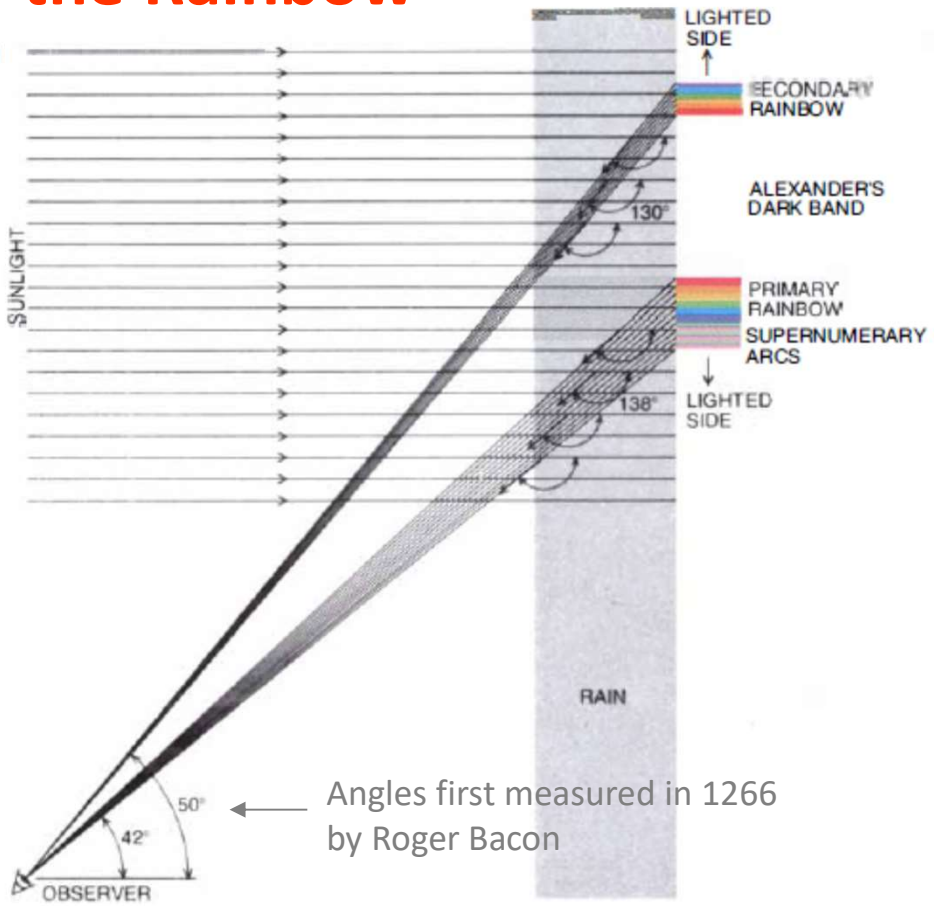

Angles first measured in 1266 by Roger Bacon

The optimum angles are slightly different for each wavelength of light, with the result that **the colors are dispersed**; note that the sequence of colors in the secondary bow is the **reverse** of that in the primary bow.

There is no single plane in which the rainbow lies; the rainbow is merely **the set of directions** along which light is scattered toward the observer.

Paths of Light through a Droplet

Rays **reflected directly** from the surface are labeled rays of Class 1; those **transmitted directly** through the droplet are designated Class 2.

The Class 3 rays emerge after **one internal reflection**; it is these that give rise to the primary rainbow.

The secondary bow is made up of Class 4 rays, which have undergone **two internal reflections**.

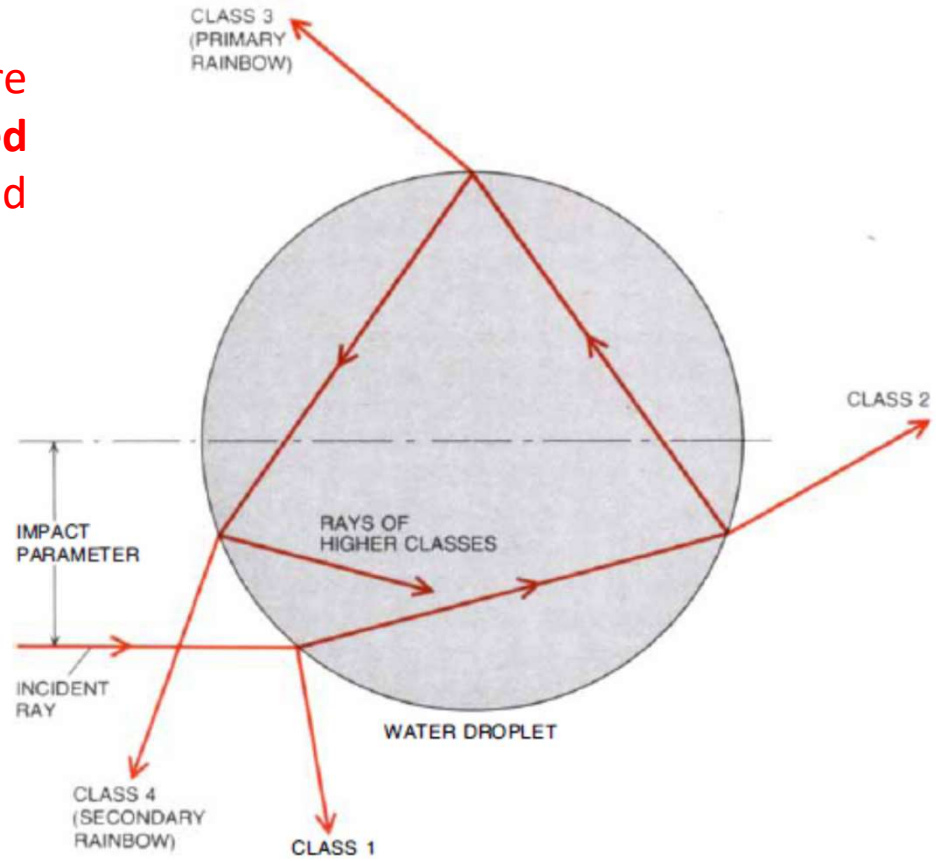

For rays of each class only one factor determines the value of the scattering angle. That factor is the **impact parameter**: the displacement of the incident ray from an axis that passes through the center of the droplet.

Rainbow Angles are Extremals of Scattering Angles

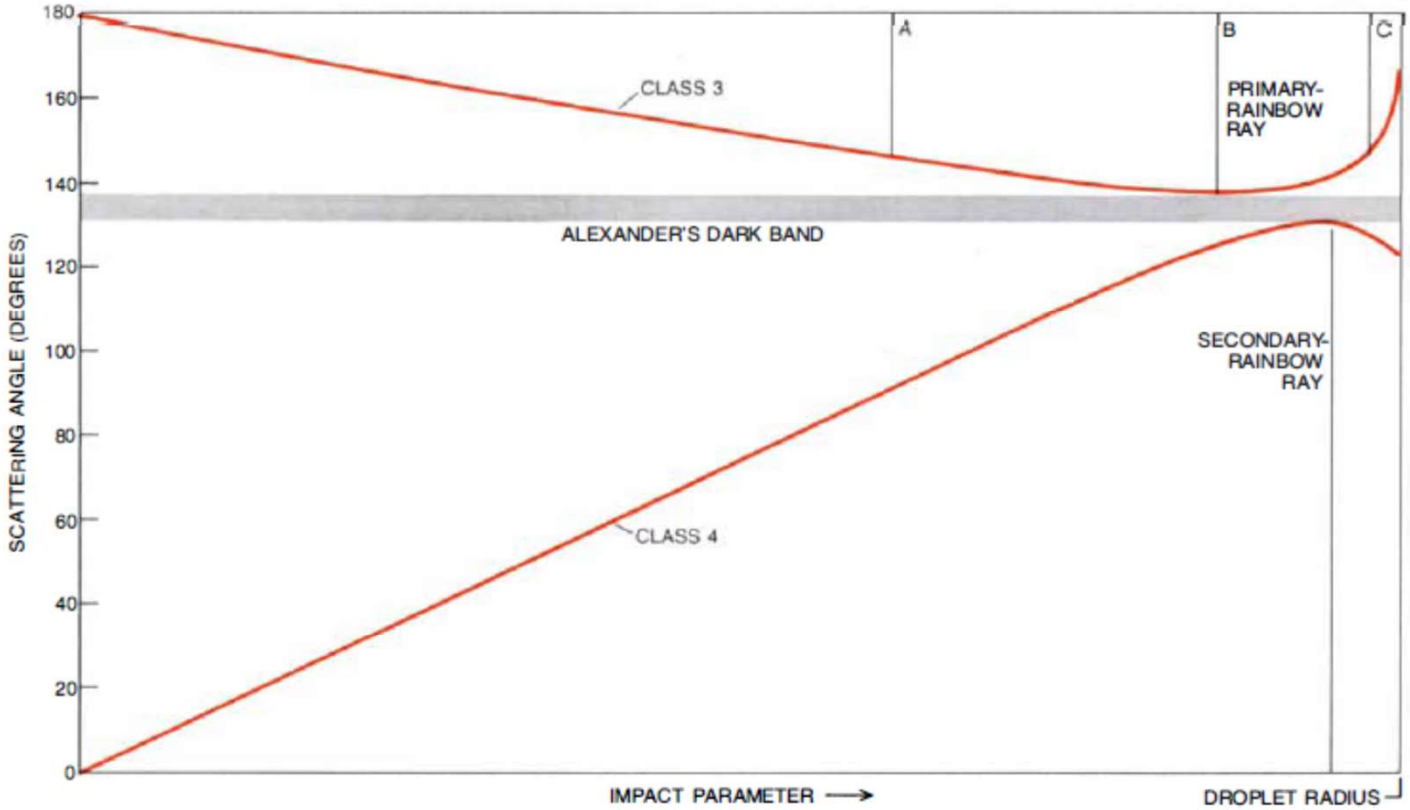

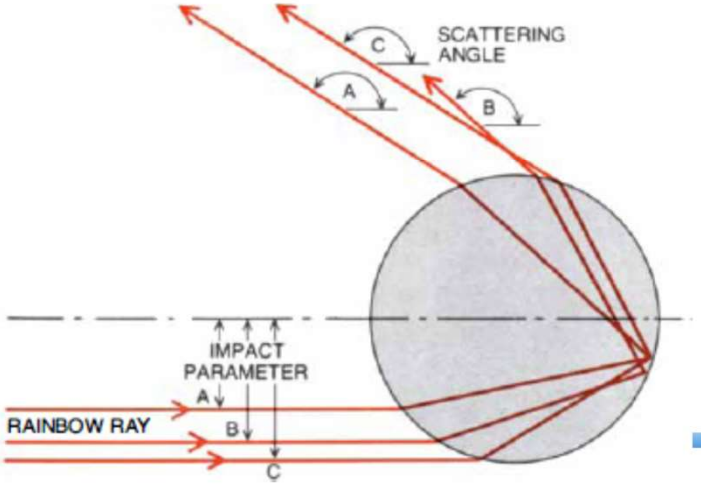

The minimum deflection is about 138 degrees, and the greatest concentration of scattered rays is to be found in the vicinity of this angle. The resulting enhancement in the intensity of the scattered light is perceived as the **primary rainbow**.

Ray Caustics

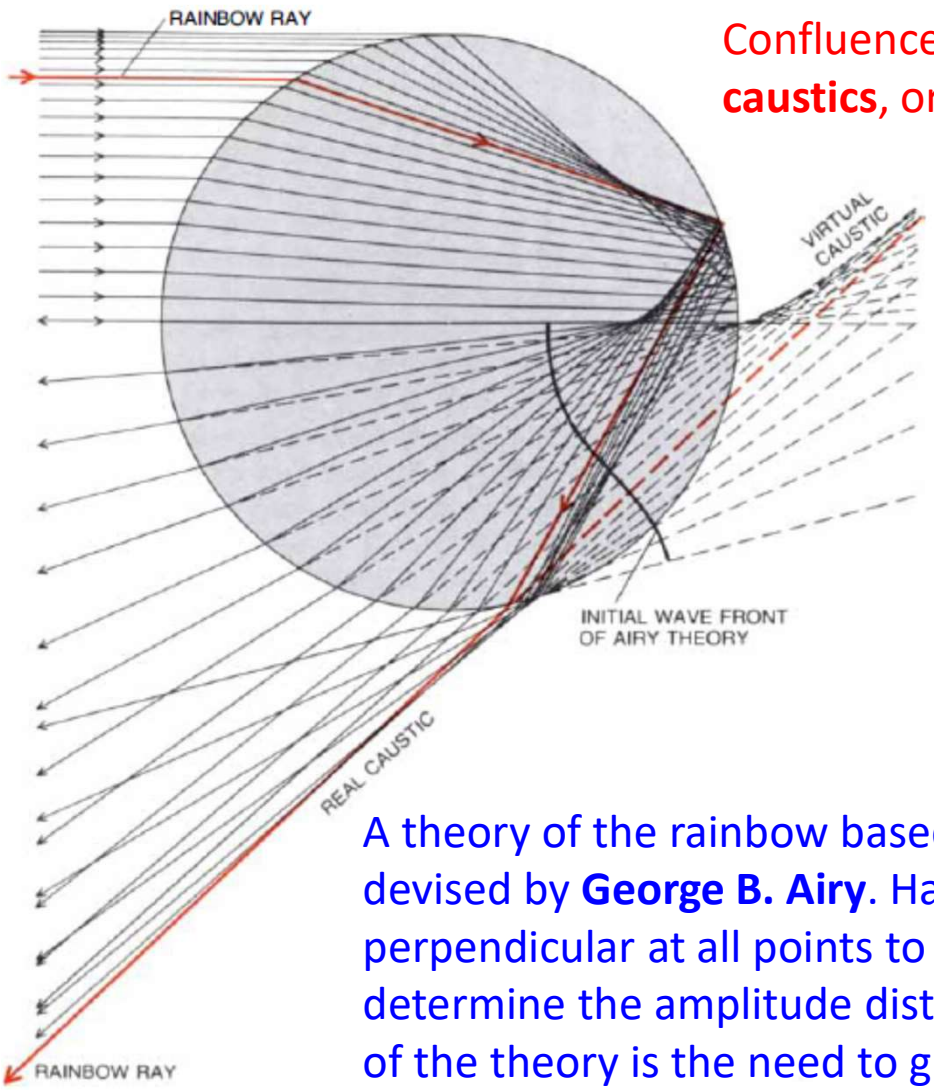

Confluence of rays scattered by a droplet gives rise to **caustics**, or "*burning curves*."

A caustic is the **envelope** of a ray system. Of special interest is the caustic of Class 3 rays, which has two branches, a real branch and a "virtual" one; the latter is formed when the rays are extended backward. When the rainbow ray is produced in both directions, it approaches the branches of this caustic.

A theory of the rainbow based on the analysis of such a caustic was devised by **George B. Airy**. Having chosen an initial wave front (a surface perpendicular at all points to the rays of Class 3) Airy was able to determine the amplitude distribution in subsequent waves. A weakness of the theory is the need to guess the amplitudes of the initial waves.

Rainbow Polarization

The angle of internal reflection for the rainbow ray **falls near Brewster's angle**.

As a result light from the rainbow has a **strong perpendicular polarization** (as it was first observed by Biot and Brewster)

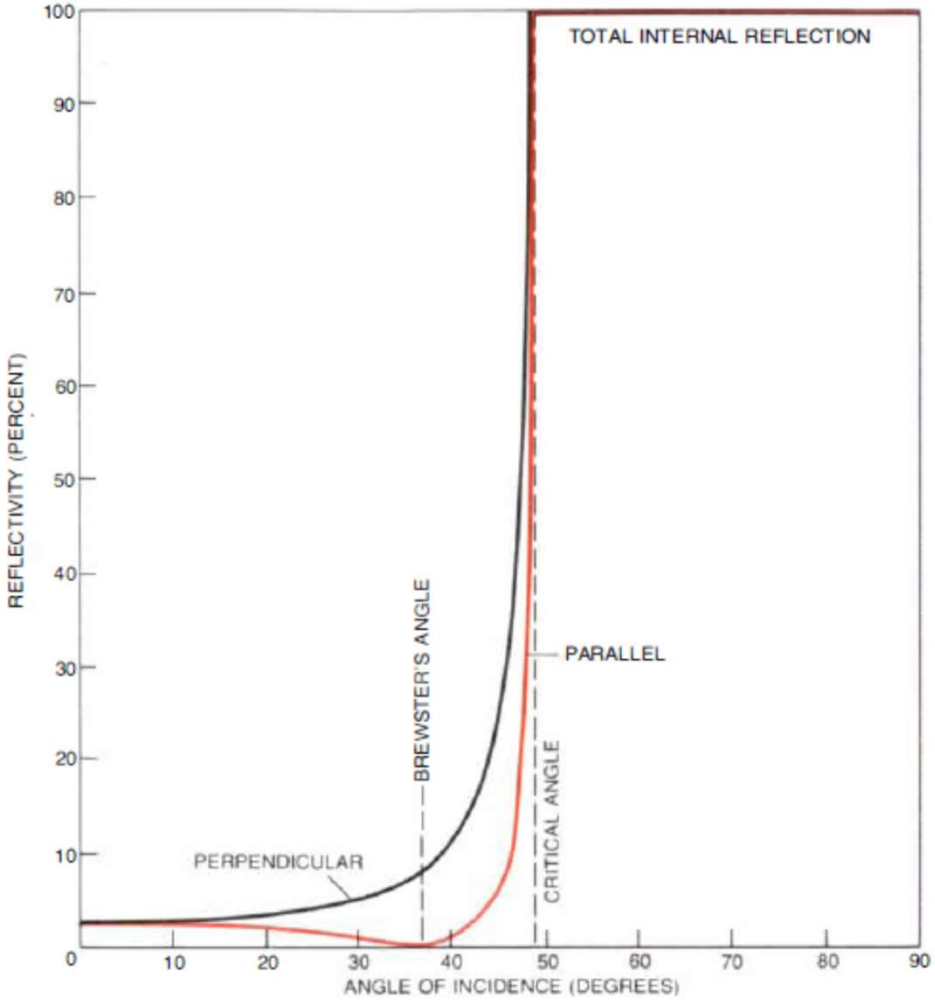

Three Early Rainbow Theories

In the geometric analysis of Descartes, intensity is **infinite** at the rainbow angle; it declines smoothly (**without supernumerary arcs**) on the lighted side and **falls off abruptly to zero** on the dark side.

The theory of Thomas Young, which is based on the interference of light waves, predicts **supernumerary arcs** but retains the **sharp transition from infinite to zero** intensity.

Airy's theory **relocates the peaks in the intensity curve** and for the first time provides (through diffraction) an explanation for **gradual fading** of the rainbow into shadow.

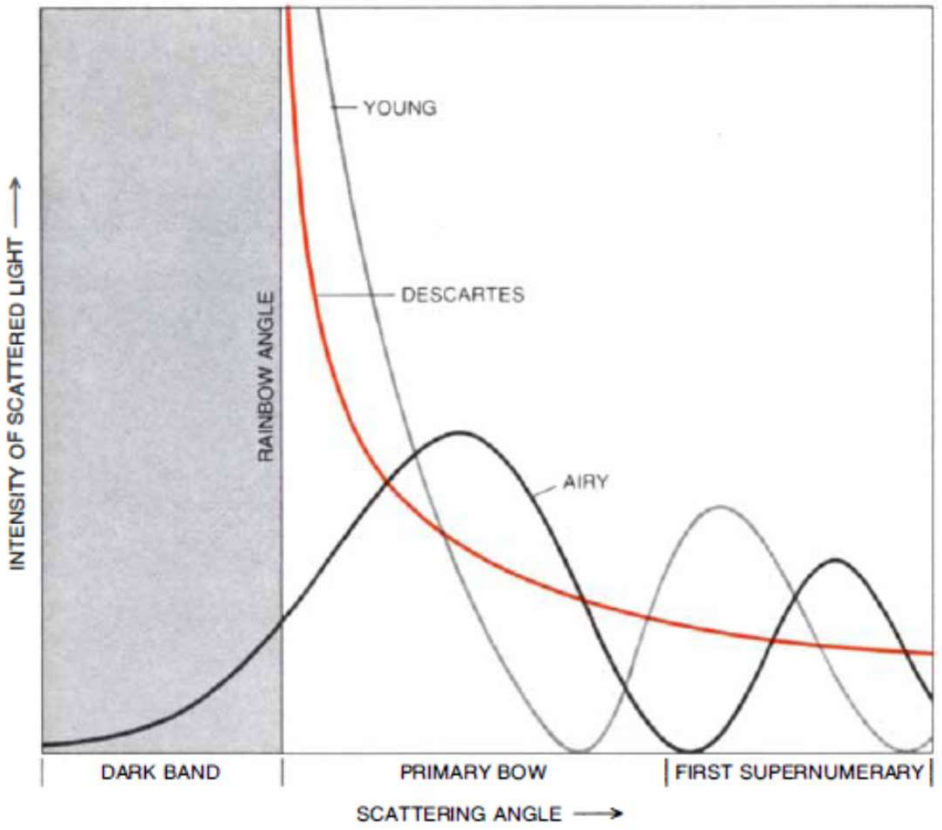

Predicted intensity as a function of scattering angle is compared for three early theories of the rainbow.

Complex Angular Momentum Theory

The domain of validity of Airy's theory was investigated by van de Hulst, who concluded that it is limited (by the assumption of a constant amplitude on the reference wavefront) to

$$\beta > 5000$$

$$\left|\theta - \theta_{\mathrm{R}}\right| < 0.5^{\circ}$$

Such limits can be greatly extended by the **complex angular momentum theory of the rainbow**, developed by H. M. Nussenzveig, which is based on the **uniform treatment of two coalescing real saddle** point that become **two complex saddle points**...

Complex Angular Momentum Theory

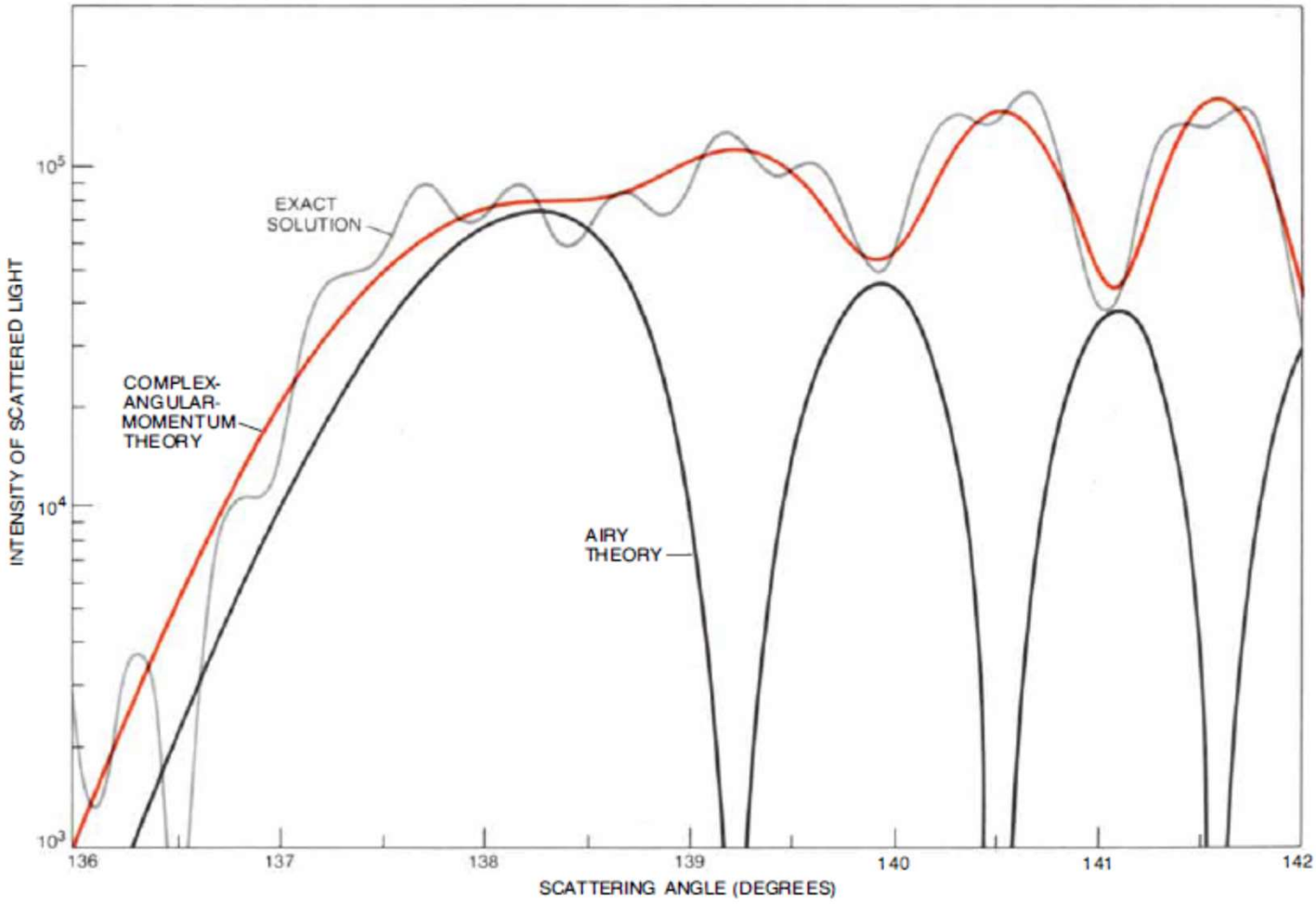

$\beta = 1500$ $N = 1.33$

The Glory

The First Reported Observation

"A cloud that covered us dissolved itself and let through the rays of the rising sun. . . . Then each of us saw his shadow projected upon the cloud. . . . What seemed most remarkable to us was ***the appearance of a halo or glory around the head, consisting of three or four small concentric circles, very brightly colored****. . . . The most surprising thing was that, of the six or seven people who were present, each of them saw the phenomenon only around the shadow of his own head, and saw nothing around other people's heads"*

(report by members of a 1748 French scientific expedition to the top of Pambamarca, now in Ecuador)

Glories from Airplanes

Glories can also be seen from inside an airplane on a daytime flight, around the shadow projected by an airplane onto the clouds.

The Glory is a Backscattering Phenomenon

Because a glory is made of light that bounced back **nearly in the same direction that it came from**, it requires a particular and serendipitous alignment of sun, observer and cloud.

Consequently, it is always seen as **a halo surrounding the observer's shadow on the cloud**.

Different colors of the spectrum come off at **slightly different angles**, producing an iridescent pattern.

A First Attempt of Explanation

Researchers first tried to attribute the phenomenon simply to **light bouncing back** inside the microscopic water droplets that compose clouds.

Light rays would bend (refract) as they entered a droplet and would get reflected in-side. Then they would bend again as they exited, going back in the direction they came from (below left).

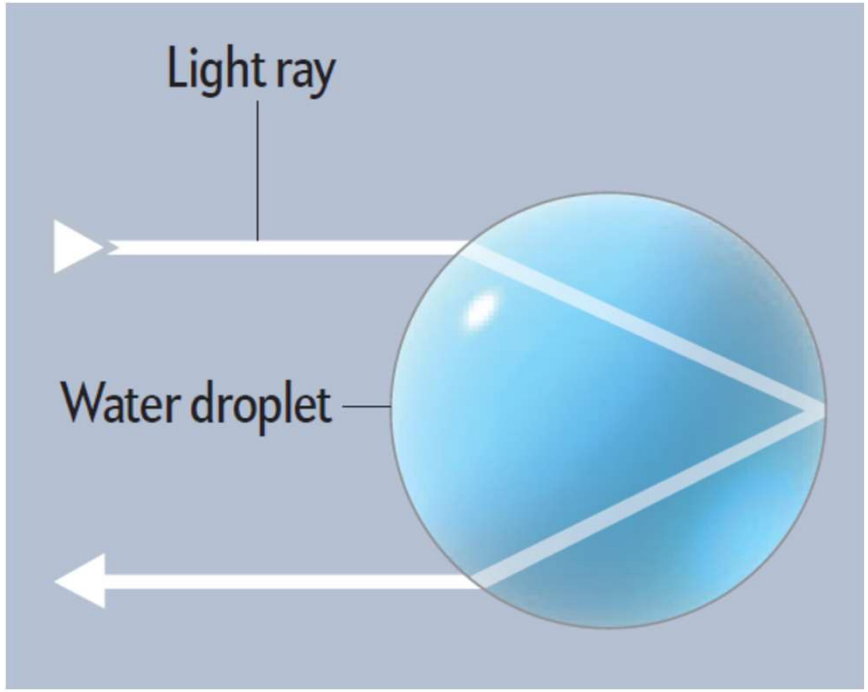

But water does not bend light rays enough for rays to go back in the exact same direction…

→ there is a 14° gap between the directions of the incident and the backscattered rays

van de Hulst Suggestion: Surface Waves

A second theory posited that light rays grazing a droplet could **temporarily turn into electromagnetic surface waves**.

By **following the curved surface** for small distances (seen exaggerated, on the right) before entering and exiting from the droplet, the light could turn by just the angle needed to return in the same direction.

This effect can take place, but it gives a relatively **minor contribution** to the overall energy seen in a glory.

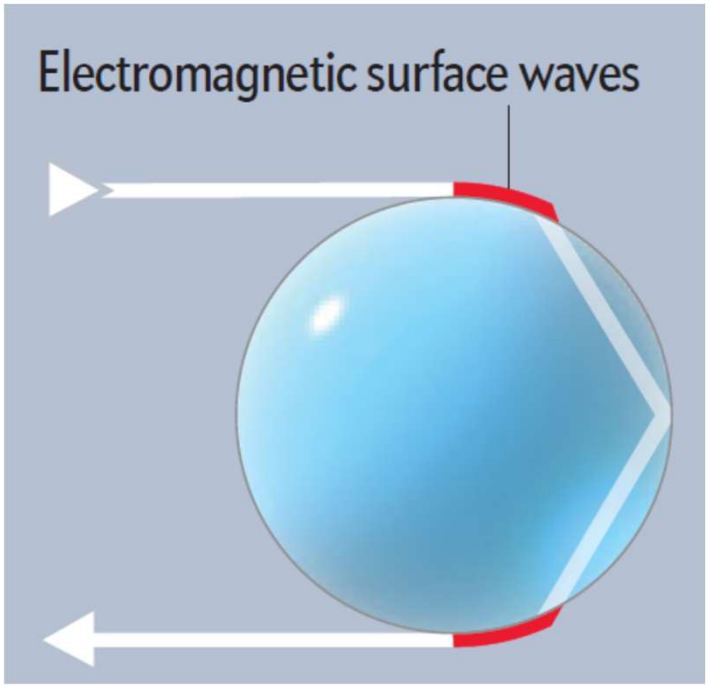

van de Hulst, 1957

Nussenzveig Theory: Light Tunneling

A mathematical theory of light scattering later explained glories through lengthy calculations but did not provide insight into the underlying physics.

H. M. Nussenzveig demonstrated that most of the light seen in a glory is the result of energy "**tunneling**" into water droplets from light rays that would otherwise seem to miss the droplets altogether.

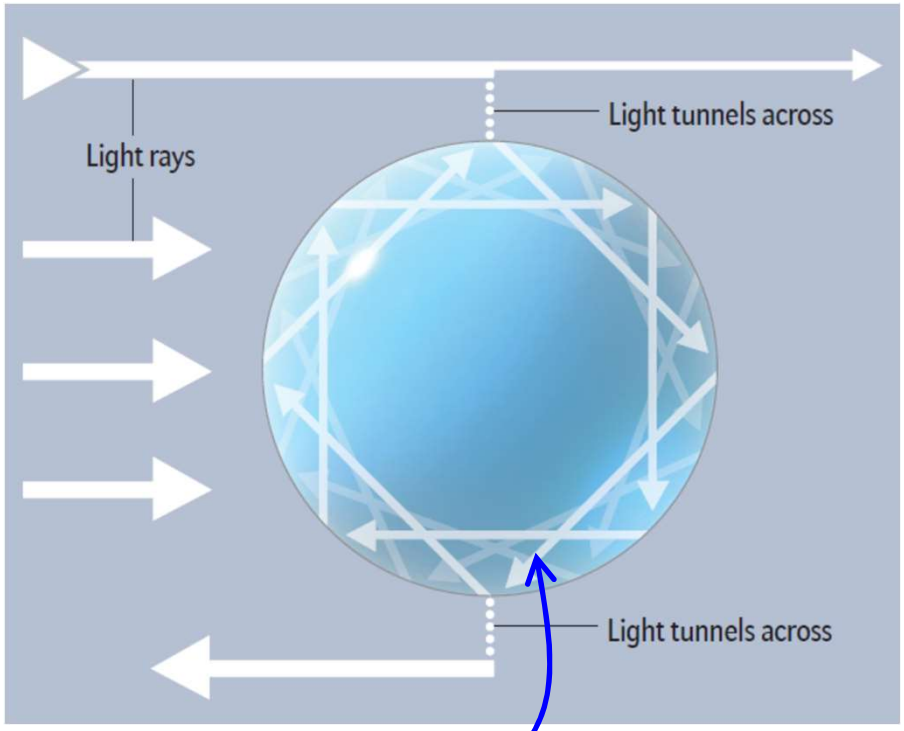

'Mie resonances' similar to the so-called 'whispering-gallery' modes

Epilogue

הַשָּׁמַיִם, מְסַפְּרִים כְּבוֹד-אֵל; וּמַעֲשֵׂה יָדָיו, מַגִּיד הָרָקִיעַ.

The heavens declare the **glory** of God;
the skies proclaim the work of his hands.

Psalm 19,1.

Grandissima mi par l'inezia di coloro che vorrebbero che Iddio avesse fatto l'universo più proporzionato alla piccola capacità del lor discorso, che all'immensa, anzi infinita, sua potenza.

To me, a great ineptitude exists on the part of those who would have it that God made the universe more in proportion to the small capacity of their reason than to His immense, His infinite, power.

Galileo Galilei, *Dialogue Concerning the Two Chief World Systems*, 1632.

References

R. F. Harrington, *Time-Harmonic Electromagnetic Fields*. Piscataway, NJ: IEEE Press, 2001.

H. C. van de Hulst, *Light Scattering from Small Particles*. New York, NY: Dover, 1957.

H. M. Nussenzveig, "High-frequency scattering by an impenetrable sphere." *Annals of Physics*, vol. 34, no. 1, pp. 23-95, 1965.

H. M. Nussenzveig, "Complex angular momentum theory of the rainbow and the glory," *Journal of the Optical Society of America*, vol. 96, no. 8, pp. 1068-1079, Aug. 1979.

References

H. M. Nussenzveig, "High-Frequency scattering by a transparent sphere. I. Direct reflection and transmission." *Journal of Mathematical Physics*, vol. 10, no. 1, pp. 82-124, 1969.

H. M. Nussenzveig, "High-frequency scattering by a transparent sphere. II. Theory of the rainbow and the glory." *Journal of Mathematical Physics*, vol. 10, no. 1, pp. 125-176, 1969.

H. M. Nussenzveig, "The theory of the rainbow." *Scientific American*, vol. 236, no. 4, pp. 116-128, Apr. 1977.

H. M. Nussenzveig, "The science of the glory." *Scientific American*, vol. 306, no. 1, pp. 68-73, Jan. 2012.